

Design study of polychromators for ITER edge Thomson scattering diagnostics

Cite as: Rev. Sci. Instrum. **79**, 10E726 (2008); <https://doi.org/10.1063/1.2969285>

Submitted: 09 May 2008 . Accepted: 21 July 2008 . Published Online: 31 October 2008

Shin Kajita, Takaki Hatae, and Yoshinori Kusama



View Online



Export Citation



Design study of polychromators for ITER edge Thomson scattering diagnostics^{a)}

Shin Kajita,^{b)} Takaki Hatae, and Yoshinori Kusama
Japan Atomic Energy Agency, Mukoyama 801-1, Naka, Ibaraki 311-0193, Japan

(Presented 13 May 2008; received 9 May 2008; accepted 21 July 2008;
 published online 31 October 2008)

In this study, we investigate designs for polychromators of the ITER edge Thomson scattering system by means of numerical calculations. For this purpose, we discuss the optimum transmission wavelength ranges of the optical filters and the optimum number of filters. Five different filter arrangements, including those with an optical notch filter to eliminate D_α emission, are compared with each other. The measurement accuracy when using a polychromator is evaluated for midplane port configuration. It is found that the optimum filter number keeping in mind the cost performance cost is 5 or 6. Moreover, the use of an optical notch filter increases the measurement accuracy by approximately 5%. © 2008 American Institute of Physics. [DOI: 10.1063/1.2969285]

I. INTRODUCTION

Incoherent Thomson scattering measurement is a standard method to measure the electron temperature T_e and density n_e . The ITER edge Thomson scattering system, whose the design is based on the yttrium aluminum garnet (YAG) Thomson scattering system in JT-60U,¹ requires a wide temperature range of 50 eV–10 keV to accurately measure T_e of less than 10% for a temporal resolution of 10 ms. Until now, to achieve the performances, the initial design of the collection optical system in the upper port plug has been conducted. A YAG laser system with 5 J output pulse energy and 100 Hz repetition frequency is now being developed.² Concerning the spectroscopic system, polychromators using optical band pass filters and avalanche photodiodes (APDs) are planned to be used.

Recently, however, another proposal has been considered, wherein the measurement system is moved to the midplane port. This proposal is from the request of H-mode pedestal research, in which the measurement in the region with the normalized radius ρ of >0.8 is important, which is >0.9 in the upper port design. It should be noted that this change may affect the designs of the collection optics system and the polychromator. In this study, we investigate polychromator designs for different configurations of laser beam and the collection optical system in the midplane port.

Polychromators with optical filters were first installed in ASDEX,³ and then, were widely used for the Thomson scattering measurements in fusion devices such as DIII-D,⁴ JT-60,¹ LHD,⁵ MAST,⁶ and JET.⁷ Most polychromator designs have been performed by considering the measurement errors. Very few designs involve numerical optimization of the filter transmission wavelength ranges. In this paper, we

design optical filters for the ITER edge Thomson scattering system using numerical simulations that are based on the method proposed in (Ref. 8). Several different filter arrangements, including those with an optical notch filters, are compared with each other in order to utilize the scattering signal, whose wavelength is less than 656 nm. The signal with wavelength shorter than 656 nm is specifically important to design the polychromators for the ITER edge Thomson scattering, although the wavelength range has not been used for YAG Thomson polychromators in other devices. The designs of the filters are optimized for the midplane configuration by taking into account the effects of the difference in the optical throughput of each APD and the density and temperature profiles of ITER for bremsstrahlung in the midplane configuration. By taking into consideration the former effect, we can determine the appropriate filter number of the measurement system, while consideration of the latter effect allows us to approximate the expected absolute measurement errors.

II. METHOD AND GEOMETRY FOR CALCULATION

In the numerical optimization process, we first determine the initial filter segment points (SEG1) and then determine the error in T_e (E_1) for SEG1 on the basis of the calculations of the Thomson scattering signal and the bremsstrahlung intensities.⁸ The second set of segment points (SEG2) is determined on the basis of SEG1; the error in T_e for SEG2 (E_2) is calculated in a manner similar to that of SEG1. The better segment set is selected on the basis of a comparison between E_1 and E_2 . The optimized segment points are deduced by performing a sufficient number of the iterative calculations of the second step using simulated annealing method,⁹ which is a generic probabilistic algorithm for global optimization. The noise power is defined as the square root of $N_0 + F_{\text{noise}}$ (photo electrons), where N_0 is the dark noise in a time slice and F_{noise} is the excess noise factor.¹⁰ In order to take into account the bremsstrahlung intensity, we consider an enhancement factor K_e , which corresponds to the difference

^{a)} Contributed paper, published as part of the Proceedings of the 17th Topical Conference on High-Temperature Plasma Diagnostics, Albuquerque, New Mexico, May 2008.

^{b)} Present address: EcoTopia Science Institute, Nagoya University, Nagoya 464-8603, Japan. Electronic mail: kajita@ees.nagoya-u.ac.jp.

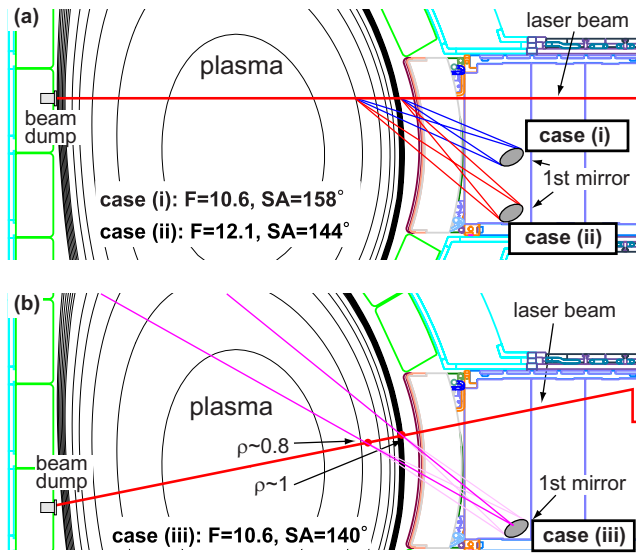


FIG. 1. (Color online) Illustrations of the ITER edge Thomson scattering measurement system in the midplane port (a) shows the case when the laser is injected horizontally, while (b) shows the case when the laser is injected diagonally.

between the theoretical and measured bremsstrahlung intensities.¹¹ The initial input values required for the calculations are $N_0=30$, $F_{\text{noise}}=2.5$, and $K_e=2$; the dark noise can be roughly estimated on the basis of its for a gain of 100, as given in Ref. 10.

Figure 1 shows illustrations of the ITER edge Thomson scattering system in the midplane port. Figure 1(a) shows the case when the laser is injected horizontally, while Fig. 1(b) shows the case when the laser is injected diagonally. In this paper, we present case studies of cases (i)–(iii), which are shown in Fig. 1. In our investigations, we have assumed that the entrance pupil is 200 mm in diameter. The important factors to be compared are the f -number of the optics F , the target of which is lower than 10, and the scattering angle (SA), which affects the spatial resolution and blueshift of the spectrum. For cases (i)–(iii), the values of F are 10.6, 12.1, and 10.6, respectively, and the SA are 158°, 144°, and 140°, respectively. Thus, the most appropriate case in terms of the f -number and SA is case (iii). In this study, as a preliminary assessment of possible midplane configuration, we consider case (iii), which is shown in Fig. 1(b), for any required calculations.

The main input parameters for the calculation are pulse width $\Delta t=30$ ns, effective path length of the plasma along the line of sight $D_{\text{brem}}=4.5$ m, laser diameter $d=5$ mm, laser pulse energy $E_i=5$ J, length of the scattering volume $\Delta L=10$ mm, solid angle $\Omega_s=0.01$, SA $\theta=129^\circ$ (for most outer channel), effective charge number $Z_{\text{eff}}=3$, and the Gaunt factor for the free-free radiation $g_{\text{eff}}=3$. The expected H-mode density and temperature profiles of ITER (Ref. 12) are used to assess the performance of the polychromator. Figure 2 shows the temperature and density profiles along the lines of sight of the midplane port (at $\rho \sim 1.0$) and upper port (at $\rho \sim 0.9$) configurations. For comparison between the midplane port and upper port cases, we can see that the lines of sight pass through the core region and the values of D_{brem} is

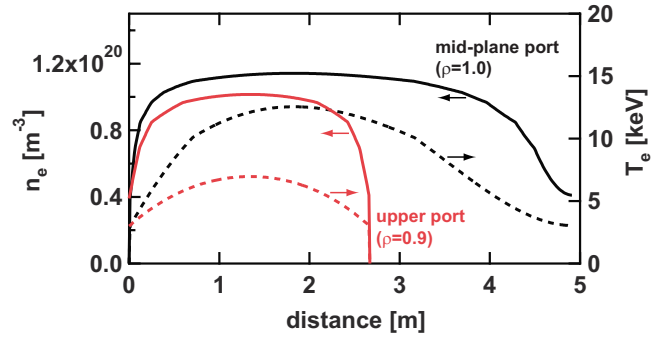


FIG. 2. (Color online) The electron density and temperature profiles along the lines of sight of the upper port (at $\rho \sim 0.9$) and midplane port (at $\rho \sim 1.0$).

greater for the midplane port case; hence, the noise level is expected to increase. In the optimization process, only the values of the core density ($1.2 \times 10^{20} \text{ m}^{-3}$), temperature (12 keV), and D_{brem} are used because we assume that the main noise source is from the core plasma in order to reduce the calculation time. In the polychromator, the transmission of the optical lens is assumed to be 95%, and the reflectivity and transmission of the filters are also assumed to be 95%. In the calculation, it is assumed that the optical throughput of the shorter wavelength channel is better.

III. RESULTS AND DISCUSSION

Figure 3(a) shows the temperature dependences of the averaged temperature errors σ_{T_e}/T_e of five different filter arrangements, i.e., cases (i)–(v). The averaged error is estimated by uniformly choosing 50 points logarithmically from $T_e=0.01$ to 20 keV, which is slightly wider than the required temperature range of $0.05 < T_e < 10$ keV. In case (i), the filter wavelength range is limited from 656 to 1064 nm. In case (ii), a filter is added below 656 nm, and in case (iii),

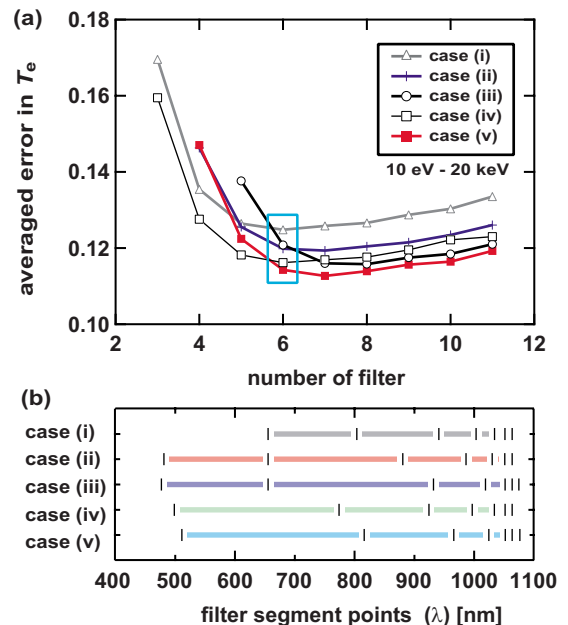


FIG. 3. (Color online) (a) Averaged error in temperature of five different filter designs, i.e., cases (i)–(v). (b) The optimized filter segment points of cases (i)–(v).

another filter is inserted above 1064 nm. In order to eliminate a strong line emission of D_α from the plasma, a segment point is set to 656 nm in cases (i)–(iii). Another way to eliminate the line emission is the use of an optical notch filter. In order to investigate the effect of the optical notch filter, we demonstrate cases in which no segment point exists at 656 nm in cases (iv) and (v). In case (v), a filter is added above 1064 nm. Figure 3(b) shows the optimized segment points of cases (i)–(v) when the number of filters is $M=6$.

It can be observed that in all the cases, the averaged error decreases with M when M is less than approximately 6 or 7. On the other hand, when M is greater, the averaged error gradually increases with M . This is because the total optical throughput of the polychromator decreases with increasing M . We think that it is appropriate to choose $M=5$ or 6 by considering the cost performance. When $M=5$ or 6, the optical notch filter increases the measurement accuracy by approximately 5%. It is also important to consider the segment point at minimum wavelength shown in Fig. 3(b). We optimized the point by setting a minimum wavelength limit of 400 nm; however, because the signal intensity around 400 nm is small, the wavelength becomes optimum around 500 nm. Since many impurity lines and deuterium Balmer lines exist in between 400 and 500 nm, it is advantageous that signals, whose wavelengths are less than 500 nm and in particular are less than D_β (486 nm), do not have a considerable impact on the system.

Figures 4(a) and 4(b) show the temperature dependences of the relative errors in electron temperature σ_{T_e}/T_e and density σ_{n_e}/n_e for $M=5$ and 6, respectively. In case (i), the error increases significantly when $T_e > 10$ keV because the Thomson signal with a wavelength shorter than 656 nm was not utilized. It can be observed that the fluctuations in temperature error in case (iii) appear to be greater than those in case (ii) and cases (iv) and (v). If an optical notch filter can be used, case (iv) with $M=5$ and case (v) with $M=6$ are appropriate. If we consider the fact that the cost of an optical notch filter is much higher than that of a normal optical filter, then case (ii) may be appropriate.

In the case of the midplane port, the measurements are obtained for the region where $\rho < 0.9$. However, the background noise level increases, as can be seen in Fig. 2, and additionally, the scattering length decreases because the distance between the magnetic surfaces became short. As a result, there is an approximately twofold increase in the measurement error of the midplane port case, as compared to the upper port case. If we consider the fact that the errors in Fig. 4 are close to the required measurement accuracy of 10% for T_e and 5% for n_e , it is thought that $\Delta L=10$ mm is necessary in the midplane port case. It is worthwhile to note that even if $\Delta L=10$ mm in the midplane port case, the spatial resolution for normalized radius becomes less than one-half of that in the case of the upper port configuration with $\Delta L=20$ mm because the distance in real space from $\rho \sim 0.9$ to 1.0 in the midplane case is approximately 20% of that in the upper port case. The measurement accuracy can be improved by shortening the pulse width. However, the laser-induced damage threshold for the in-vessel mirror decreases with the

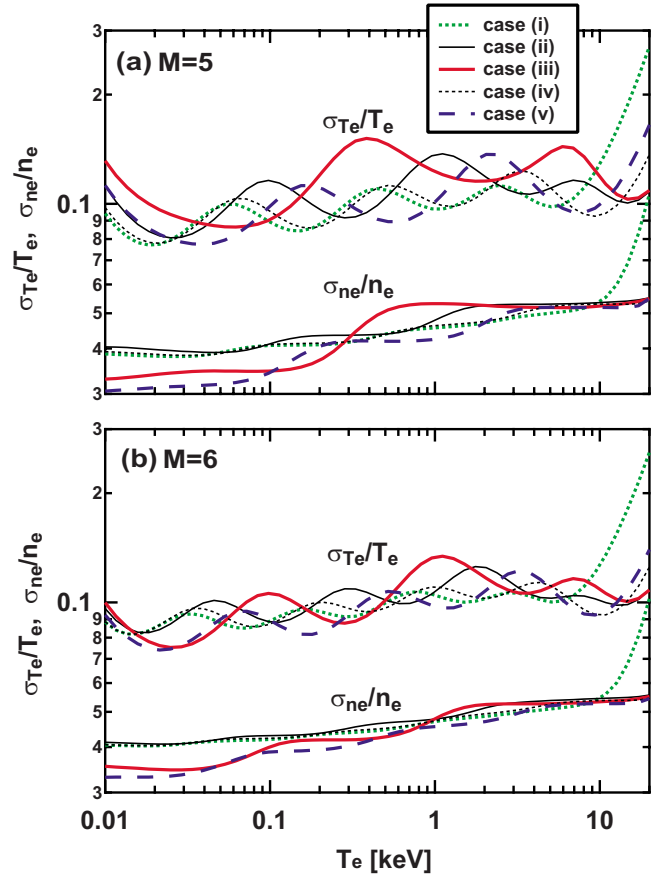


FIG. 4. (Color online) Temperature dependences of the relative estimated errors in T_e and n_e for (a) $M=5$ and (b) $M=6$ in the five cases (i)–(v) presented in Fig. 3.

pulse width;¹³ hence, it may be difficult to shorten the pulse width drastically such as in the case of LIDAR, whose pulse width is expected to be ~ 300 ps.

It is necessary to consider the effects of several factors that may affect the segment points. We discuss these factors while considering case (ii) with $M=6$. We determined the optimum segment points by changing the background density, temperature, and scattering angle, which changes slightly with each line of sight; however, it was found that these factors are minority factors and do not have a considerable effect on the segment points. The only important factor that affects the points is the order of the filters. Let us compare two cases: (a) the case where the detector with the short wavelength has better throughput and (b) the case where the detector with the long wavelength has better throughput. The measurement accuracy in case (b) is slightly better (approximately 2%) than that in case (a); the segment points in case (b) shifted to a shorter wavelength, as compared to case (a) (shifted ~ 48 nm around 850 nm at maximum). These differences may be significant when fabricating filters. The number of possible permutations of the filter order is 720 when $M=6$. Thus, we can find an optimum permutation with a smaller error by investigating all the possible permutations. However, this will be covered in a future study.

IV. CONCLUSIONS

In this study, we have investigated designs for the polychromators of the ITER edge Thomson scattering system in midplane port configuration. The transmission wavelength ranges of the optical filters of the polychromators are optimized by comparing several different arrangements. We concluded that a filter number of 5 or 6 is the most optimal number keeping in mind the cost performance. For example, when the filter number is 6, it is necessary to add an optical filter below 656 nm, which corresponds to the wavelength of a strong radiation of D_α . We found that the use of an optical notch filter for extracting D_α increases the measurement accuracy by approximately 5%. For midplane port configuration, it is concluded that it is necessary to have a scattering length L of at least 10 mm to satisfy the measurement accuracy required under the present calculation conditions, where the laser pulse energy is 5 J and the width is 30 ns.

ACKNOWLEDGMENTS

The authors thank Dr. O. Naito of JAEA for helpful discussion and comments.

¹T. Hatae, A. Nagashima, T. Kondoh, S. Kitamura, T. Kashiwabara, H. Yoshida, O. Naito, K. Shimizu, O. Yamashita, and T. Sakuma, *Rev. Sci.*

Instrum. **70**, 772 (1999).

²T. Hatae, M. Nakatsuka, H. Yoshida, K. Ebisawa, Y. Kusama, K. Sato, A. Katsunuma, H. Kubomura, and K. Shinobu, *Fusion Sci. Technol.* **51**, 58 (2007).

³H. Röhr, K. H. Steuer, H. Murmann, D. Meisel, "Periodic multichannel Thomson scattering system in ASDEX," IPP-Report No. III/121 B 1987.

⁴T. N. Carlstrom, J. C. DeBoo, R. Evanko, C. M. Greenfield, C.-L. Hsieh, R. T. Snider and P. Trost, *Rev. Sci. Instrum.* **61**, 2858 (1990).

⁵K. Narihara, K. Yamauchi, I. Yamada, T. Minami, K. Adachi, A. Ejiri, Y. Hamada, K. Ida, H. Iguchi, K. Kawahata, T. Ozaki and K. Toi, *Fusion Eng. Des.* **34**, 67 (1997).

⁶R. Scannell, M. J. Walsh, P. G. Carolan, N. J. Conway, A. C. Darke, M. R. Dunstan, D. Hare, and S. L. Prunty, *Rev. Sci. Instrum.* **77**, 10E510 (2006).

⁷R. Pasqualotto, P. Nielsen, C. Gowers, M. Beurskens, M. Kempenaars, T. Carlstrom, D. Johnson, and J.-E. Contributors, *Rev. Sci. Instrum.* **75**, 3891 (2004).

⁸O. Naito, H. Yoshida, S. Kitamura, T. Sakuma, and Y. Onose, *Rev. Sci. Instrum.* **70**, 3780 (1999); S. Kajita, T. Hatae, and O. Naito, "Optimization of optical filters for ITER edge Thomson scattering diagnostics," *Fusion Eng. Des.* (submitted).

⁹W. H. Press, S. A. Teukolsky, W. T. Vetterling, and B. P. Flannery, *Numerical Recipes in C*, 1st ed. (Cambridge University Press, Cambridge, 1988).

¹⁰R. Pasqualotto, P. Nielsen, and L. Giudicotti, *Rev. Sci. Instrum.* **72**, 1134 (2001).

¹¹P. Nielsen, Proceedings of the course held in Varenna Como, Italy, 1982 (unpublished), pp. 244–246.

¹²G. W. Pacher, H. D. Pacher, G. Janeschitz, A. S. Kukushkin, and G. Pereverzev, *Plasma Phys. Controlled Fusion* **46**, A257 (2004).

¹³S. Kajita, T. Hatae, and V. Voitsenya, *J. Plasma Fusion Res.* **3**, 032 (2008).